

Research Article

Pretargeted Immuno–Positron Emission Tomography Imaging of Carcinoembryonic Antigen–Expressing Tumors with a Bispecific Antibody and a ^{68}Ga - and ^{18}F -Labeled Hapten Peptide in Mice with Human Tumor Xenografts

Rafke Schoffelen¹, Robert M. Sharkey³, David M. Goldenberg³, Gerben Franssen¹, William J. McBride⁴, Edmund A. Rossi⁵, Chien-Hsing Chang^{4,5}, Peter Laverman¹, Jonathan A. Disselhorst¹, Annemarie Eek¹, Winette T.A. van der Graaf², Wim J.G. Oyen¹, and Otto C. Boerman¹

Abstract

^{18}F -Fluorodeoxyglucose (^{18}F -FDG) is the most common molecular imaging agent in oncology, with a high sensitivity and specificity for detecting several cancers. Antibodies could enhance specificity; therefore, procedures were developed for radiolabeling a small (~1451 Da) hapten peptide with ^{68}Ga or ^{18}F to compare their specificity with ^{18}F -FDG for detecting tumors using a pretargeting procedure. Mice were implanted with carcinoembryonic antigen (CEA; CEACAM5)–expressing LS174T human colonic tumors and a CEA-negative tumor, or an inflammation was induced in thigh muscle. A bispecific monoclonal anti-CEA \times anti-hapten antibody was given to mice, and 16 hours later, 5 MBq of ^{68}Ga - or ^{18}F -labeled hapten peptides were administered intravenously. Within 1 hour, tissues showed high and specific targeting of ^{68}Ga -IMP-288, with $10.7 \pm 3.6\%$ ID/g uptake in the tumor and very low uptake in normal tissues (e.g., tumor-to-blood ratio of 69.9 ± 32.3), in a CEA-negative tumor ($0.35 \pm 0.35\%$ ID/g), and inflamed muscle ($0.72 \pm 0.20\%$ ID/g). ^{18}F -FDG localized efficiently in the tumor ($7.42 \pm 0.20\%$ ID/g) but also in the inflamed muscle ($4.07 \pm 1.13\%$ ID/g) and in several normal tissues; thus, pretargeted ^{68}Ga -IMP-288 provided better specificity and sensitivity. Positron emission tomography (PET)/computed tomography images reinforced the improved specificity of the pretargeting method. ^{18}F -labeled IMP-449 distributed similarly in the tumor and normal tissues as the ^{68}Ga -labeled IMP-288, indicating that either radiolabeled hapten peptide could be used. Thus, pretargeted immuno-PET does exceptionally well with short-lived radionuclides and is a highly sensitive procedure that is more specific than ^{18}F -FDG-PET. *Mol Cancer Ther*; 9(4); 1019–27. ©2010 AACR.

Introduction

Radiolabeled antibody targeting of tumor-associated antigens often requires several days for adequate visualization of tumors due to the slow pharmacokinetics and accretion of intact antibodies in tumors (1). The use of antibody fragments and engineered antibody formats [such as F(ab')₂, Fab', diabodies, minibodies, or scFv] has improved radioimmunodetection only to a limited

extent. Tumor uptake of most antibody fragments is much lower than that of an IgG, resulting in reduced signal strength in the tumors, which can contribute to uncertainties in interpretation (2). Pretargeting techniques were developed to improve radioimmunotargeting of tumors (3–5). In pretargeting, an unlabeled bifunctional reagent with affinity for the tumor and a small radiolabeled molecule is given in advance of the radiolabeled compound (4–6). Two main antibody-based pretargeting approaches can be distinguished: strategies that use (strept)avidin and biotin and those that use bispecific monoclonal antibodies (bsMAB). The disadvantages of the biotin-avidin-based approaches are the immunogenicity of (strept)avidin and the need for a clearing agent to remove the antibody conjugate from the blood (4). A bsMAB, which can be humanized to reduce immunogenicity, will bind a tumor-associated antigen and a hapten. Coupling two haptens together improves peptide uptake and stability by a process known as affinity enhancement (7). Chelate-metal complexes, such as diethylenetriaminepentaacetic acid (DTPA)–In, have been used as haptens (8). More recently, peptides

Authors' Affiliations: Departments of ¹Nuclear Medicine and ²Medical Oncology, Radboud University Nijmegen Medical Centre, Nijmegen, the Netherlands; ³Garden State Cancer Center, Center for Molecular Medicine and Immunology, Belleville, New Jersey; and ⁴IBC Pharmaceuticals, Inc.; ⁵Immunomedics, Inc., Morris Plains, New Jersey

Corresponding Author: Rafke Schoffelen, Department of Nuclear Medicine, Radboud University Nijmegen Medical Centre, P.O. Box 9101, 6500 HB Nijmegen, the Netherlands. Phone: 31-24-3619097; Fax: 31-24-3618942. E-mail: r.schoffelen@nuumed.umcn.nl

doi: 10.1158/1535-7163.MCT-09-0862

©2010 American Association for Cancer Research.

substituted with the hapten, histamine-succinyl-glycine (HSG), in combination with anti-HSG bsMAbs have provided a more flexible system because these HSG-substituted peptides can be conjugated with various chelating moieties [DTPA; 1,4,7,10-tetraazacyclododecane-*N,N',N'',N'''*-tetraacetic acid (DOTA); N_3S chelates; etc.]. Consequently, they can be labeled with a wide variety of radionuclides, such as ^{111}In and $^{99\text{m}}\text{Tc}$, for single-photon emission computed tomography (CT) imaging (6), with ^{124}I for positron emission tomography (PET) imaging (9, 10), or with ^{131}I , ^{90}Y , and ^{177}Lu for pretargeted radioimmunotherapy (11).

Previous studies illustrated the enhanced sensitivity of pretargeted imaging for detecting cancer (6, 10, 12), with superior results of pretargeting compared with the directly radiolabeled antibody fragment. In a micro-metastatic human colon cancer model, tumor nodules no larger than 0.3 mm in diameter were detected in the lungs of athymic mice with the ^{124}I -labeled di-HSG peptide (12). This study highlighted the exceptional sensitivity of the pretargeting procedure, but herein, we also wanted to examine the specificity of pretargeting and therefore included a model of sterile inflammation.

Earlier studies were done with ^{124}I because it was commercially available and the chemistry for iodination was well known. However, ^{124}I is not an ideal radionuclide for PET imaging due to its high-energy positrons and considerable expense. Its long half-life ($t_{1/2} = 4.2$ days) has been an advantage for directly radiolabeled antibodies that require extended periods for adequate contrast to develop, which only takes 1 hour with pretargeting, making this method more amenable to short-lived positron emitting radionuclides. There are currently two radionuclides with exceptional imaging properties for PET (i.e., ^{68}Ga and ^{18}F), and their half-lives are well matched with the pharmacokinetics of the radiolabeled peptide (^{68}Ga $t_{1/2} = 68$ minutes; ^{18}F $t_{1/2} = 110$ minutes). ^{68}Ga is a relative newcomer to nuclear medicine, and in addition to its physical properties, it is readily available in a nearly carrier-free state from an in-house $^{68}\text{Ge}/^{68}\text{Ga}$ generator.

Herein, we report the first pretargeting studies with this ^{68}Ga -labeled peptide. ^{18}F has been the gold standard for PET studies. It is abundantly available and inexpensive, but the chemistry involved in preparing labeled products can be challenging. We recently reported a simplified approach for preparing ^{18}F -labeled peptides that involves the formation of ^{18}F -aluminum complexes that can then be simply bound to a chelate on a peptide (13). Thus, another objective of this study was to compare a ^{68}Ga -labeled and an ^{18}F -labeled peptide with pretargeting.

In summary, we show the feasibility of using ^{68}Ga - or ^{18}F -labeled di-HSG peptides in pretargeting and further show the improved specificity afforded by pretargeting by including a comparison of ^{18}F -fluorodeoxyglucose (^{18}F -FDG) and an inflammation model.

Materials and Methods

Pretargeting reagents TF2, IMP-288, and IMP-449

The bsMAb TF2 and the peptides IMP-288 and IMP-449 were provided by Immunomedics, Inc. TF2 is an engineered trivalent bispecific antibody composed of a humanized anti-HSG Fab fragment derived from the 679 anti-HSG monoclonal antibodies (14) and two humanized anti-carcinoembryonic antigen (CEA) Fab fragments derived from the hMN-14 antibody or labetuzumab (14, 15), formed into a 157×10^3 Da protein by the Dock-and-Lock procedure (16, 17). The immunoreactive fraction of TF2 for binding to CEA, determined in a Lindmo assay (18) on fixed LS174T cells, exceeded 85%. Gel filtration chromatography showed that TF2 could bind >90% of ^{68}Ga -IMP-288 peptide.

IMP-288 was synthesized and purified as described by McBride et al. (10). It is a DOTA-conjugated D-Tyr-D-Lys-D-Glu-D-Lys tetrapeptide in which both lysine residues are substituted with a HSG moiety via their ϵ -amino group: DOTA-D-Tyr-D-Lys(HSG)-D-Glu-D-Lys(HSG)- NH_2 (Fig. 1A). A similar peptide, IMP-449, was conjugated with 1,4,7-tri-azacyclononane-*N,N',N'''*-triacetic acid (NOTA), instead of DOTA, to facilitate labeling with ^{18}F (Fig. 1B). To improve the conjugation of the NOTA chelator, an alanine residue was used as a spacer (13).

TF2 was labeled with ^{125}I (Perkin-Elmer) by the iodogen method (19) to a specific activity of 58 MBq/nmol. ^{125}I -labeled TF2 was purified by eluting the reaction mixture with PBS and 0.5% (w/v) bovine serum albumin (Sigma Chemical) on a PD-10 column (GE Healthcare Bio-Sciences AB).

Labeling of IMP-288 or IMP-449

IMP-288 was labeled with ^{111}In (Covidien) at 32 MBq/nmol under strict metal-free conditions. Briefly, 11 MBq ^{111}In was added to 12 μg IMP-288 in 0.25 mol/L ammonium acetate (NH_4Ac) buffer (pH 5.6), and after 20 min at 95°C, 10 μL of 50 mmol/L EDTA were added to complex any unbound ^{111}In .

IMP-288 was labeled with ^{68}Ga eluted from a TiO-based 1,110 MBq $^{68}\text{Ge}/^{68}\text{Ga}$ generator (Cyclotron Co. Ltd.) using 0.1 mol/L ultrapure HCl (J.T. Baker). Five 1-mL fractions were collected, and the second fraction was used for labeling the peptide. One volume of 1.0 mol/L HEPES buffer (pH 7.0) was added to 3.4 nmol IMP-288. Four volumes of ^{68}Ga eluate (380 MBq) were added, and the mixture was heated at 95°C for 20 min. EDTA (50 mmol/L) was added to a final concentration of 5 mmol/L to complex the nonchelated $^{68}\text{Ga}^{3+}$, followed by purification on a 1-mL Oasis HLB cartridge (Waters). After washing the cartridge with water, the peptide was eluted with 25% ethanol.

IMP-449 was labeled with ^{18}F as described by McBride et al. (13). [^{18}F]Fluoride (555–740 MBq; B.V. Cyclotron VU) was eluted from a QMA cartridge with 0.4 mol/L KHCO_3 . Four 200- μL fractions were collected

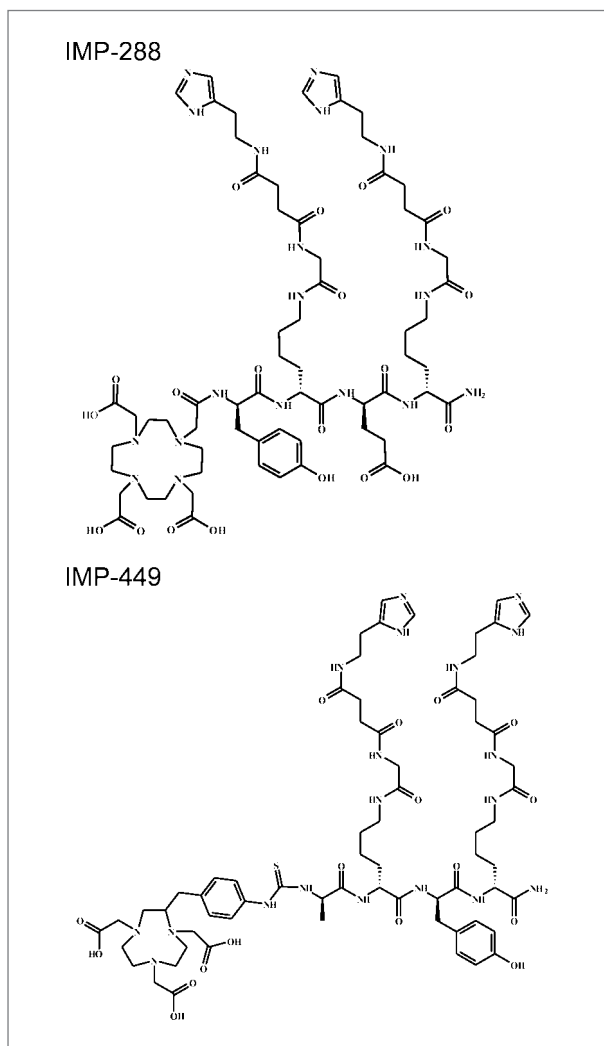


Figure 1. Chemical structures of IMP-288 and IMP-449. Both are Tyr-D-Lys-D-Glu-D-Lys tetrapeptides in which both lysine residues are substituted with a HSG moiety via their ϵ -amino group. IMP-288 is conjugated with DOTA, and IMP-449 is conjugated with NOTA.

in vials containing 3 μ L of 2 mmol/L AlCl_3 in 0.1 mol/L sodium acetate buffer (pH 4). The fraction with highest activity was used. The $\text{Al}[\text{}^{18}\text{F}]^{2+}$ activity was added to a vial containing IMP-449 (230 μ g) and ascorbic acid (10 mg). The mixture was incubated at 100°C for 15 min and then purified by reversed-phase high-performance liquid chromatography (Phenomenex Onyx monolithic C18 column) using a linear gradient of 97% A to 100% B in 30 min [buffer A: 0.1% trifluoroacetic acid (TFA) in water; buffer B: 0.1% TFA in acetonitrile; flow rate: 3 mL/min]. After adding one volume of water, the peptide was purified on a 1-mL Oasis HLB cartridge. After washing with water, the radiolabeled peptide was eluted with 50% ethanol.

Quality control of the radiolabeled preparations

Radiochemical purity was determined using instant TLC on silica gel strips (Pall Life Sciences) using

0.1 mol/L citrate buffer (pH 6.0) as the mobile phase. The colloid content of the radiolabeled peptide was determined by instant TLC on silica gel strips using a 1:1 (v/v) solution of 0.15 mol/L NH_4Ac (pH 5.5) and methanol as the mobile phase.

^{111}In -IMP-288, ^{68}Ga -IMP-288, and ^{18}F -IMP-449 were analyzed by reversed-phase high-performance liquid chromatography (Agilent 1100 series, Agilent Technologies) on a RP C_{18} column (Alltima, 5 μ m, 4.6 \times 250 mm, Alltech) using a flow rate of 1.0 mL/min with a linear gradient of 97% A and 3% to 100% B over 15 min (buffer A: 0.1% TFA in water; buffer B: 0.1% TFA in acetonitrile). Radiochemical purity of ^{125}I -TF2, ^{111}In -IMP-288, ^{68}Ga -IMP-288, and ^{18}F -IMP-449 preparations always exceeded 95%.

Animal experiments

All studies were approved by the institutional Animal Welfare Committee of the Radboud University Nijmegen Medical Centre and conducted in accordance with their guidelines (revised Dutch Act on Animal Experimentation, 1997). Male nude BALB/c mice (6–8 wk old), weighing 20 to 25 g, received a s.c. injection with 0.2 mL of a suspension of 1×10^6 LS174T, a CEA-expressing human colon carcinoma cell line (CCL-188; passage 7; American Type Culture Collection). In some studies, animals were coimplanted with SK-RC 52 cells, a human renal cancer cell line that is negative for CEA (20). The CEA production of LS174T in the American Type Culture Collection seed stock was 1,944 ng per million cells in 10 d. Homogenized tissue of s.c. LS174T and SK-RC 52 tumors during 10 d, grown in nude BALB/c mice, showed that the LS174T tumor had a CEA content of 17,745 ng per million cells, whereas the SK-RC 52 tumor had no detectable CEA content. Studies were initiated when the tumors reached a size of about 0.1 to 0.3 g.

In separate studies, animals bearing an LS174T xenograft in one hind leg were injected in the other hind limb muscle with 50 μ L turpentine to induce an inflammatory reaction (21).

TF2 was given i.v., and 16 h later, radiolabeled IMP-288 was given in 0.2 mL. This interval was shown previously to be sufficient to clear TF2 from the circulation (15). In some studies, ^{125}I -TF2 (0.4 MBq) was coinjected with unlabeled TF2. One hour after the injection of ^{68}Ga -labeled peptide, and 2 h after injection of ^{18}F -IMP-449, mice were euthanized by CO_2/O_2 , and blood was obtained by cardiac puncture.

PET images were acquired with an Inveon animal PET/CT scanner (Siemens Preclinical Solutions) with an intrinsic spatial resolution of 1.5 mm (22). The animals were placed in a supine position. PET emission scans were acquired for 15 min, preceded by CT scans for anatomic reference (spatial resolution, 113 μ m; 80 kV; 500 μ A; exposure time, 300 ms).

Scans were reconstructed using Inveon Acquisition Workplace software (version 1.2; Siemens Preclinical

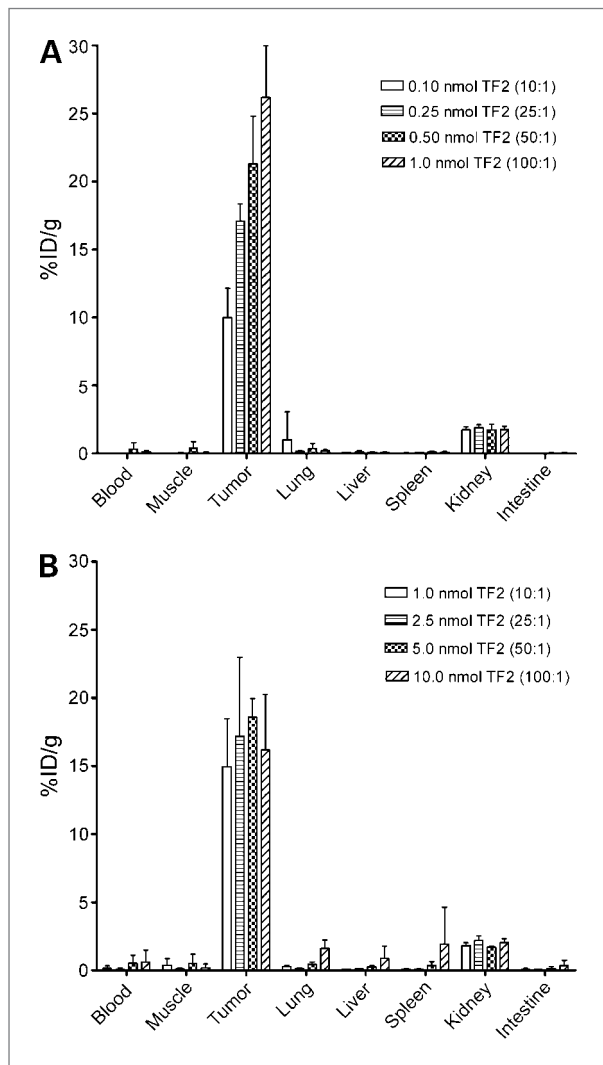


Figure 2. Biodistribution of ^{111}In -IMP-288 1 h after i.v. injection, following pretargeting with escalating doses of TF2 in BALB/c nude mice with a s.c. CEA-expressing LS174T tumor. Two peptide doses were tested: 0.1 nmol ^{111}In -IMP-288 (A) and 0.10 nmol ^{111}In -IMP-288 (B). Values are given as means \pm SD ($n = 5$).

Solutions) using a three-dimensional ordered subset expectation maximization/maximum a posteriori algorithm with the following parameters: matrix, $256 \times 256 \times 159$; pixel size, $0.43 \times 0.43 \times 0.8 \text{ mm}^3$; and maximum a posteriori prior β , 0.5.

After imaging, tumor and organs of interest were dissected, weighed, and counted in a gamma counter with appropriate energy windows for ^{125}I , ^{111}In , ^{68}Ga , or ^{18}F . The percentage injected dose per gram tissue (% ID/g) was calculated.

Statistical analysis

All mean values are given \pm SD. Statistical analysis was done using a nonparametric, two-tailed Mann-Whitney test using GraphPad InStat software (version

4.00; GraphPad Software). The level of significance was set at $P < 0.05$.

Results

Dose optimization

The effect of the TF2 dose on tumor targeting with a fixed amount of IMP-288 (0.01 or 0.1 nmol; 15 or 150 ng, respectively) was determined. Groups of five mice were injected i.v. with 0.10, 0.25, 0.50, or 1.0 nmol TF2, labeled with a trace amount of ^{125}I (0.4 MBq). Two hours after injection of ^{111}In -IMP-288 (0.01 nmol, 0.4 MBq), the biodistribution of the radiolabels was determined.

TF2 cleared rapidly from blood and normal tissues. Eighteen hours after injection, the blood concentration was $<0.45\%$ ID/g at all TF2 doses tested. TF2 tumor uptake was 3.5% ID/g, independent of TF2 dose up to 1.0 nmol (data not shown). At all TF2 doses, ^{111}In -IMP-288 accumulated effectively in the tumor, with increasing uptake associated with higher TF2 doses (Fig. 2A). At the 0.01 nmol ^{111}In -IMP-288 dose, tumor uptake peaked at $26.2 \pm 3.8\%$ ID/g. With 0.01 nmol of IMP-288, the highest tumor targeting and tumor-to-blood ratios were achieved with 1.0 nmol TF2 (TF2-to-IMP-288 molar ratio = 100:1). The kidneys had the highest normal organ accretion of ^{111}In -IMP-288 ($1.75 \pm 0.27\%$ ID/g); all other normal tissues had very low uptake.

With ^{68}Ga -labeled IMP-288, a minimum of 5 to 10 MBq ^{68}Ga was required for PET imaging done 1 hour after injection. At a maximum specific activity of 50 to 125 MBq/nmol at the time of injection, at least 0.1 to 0.25 nmol of ^{68}Ga -IMP-288 had to be administered. A separate group of LS174T-bearing mice received the same TF2-to-IMP-288 molar ratios as were tested above, but with 0.1 nmol IMP-288, 1.0, 2.5, 5.0, or 10.0 nmol of TF2 were administered. The percent uptake of TF2 in the tumor decreased from $3.21 \pm 0.61\%$ ID/g at the 1.0 nmol dose to $1.16 \pm 0.27\%$ ID/g with 10.0 nmol, suggesting that the antigen in the tumor was saturated. In contrast to the results at the 0.01 nmol dose, tumor uptake with 0.1 nmol ^{111}In -IMP-288 was not affected by the TF2 dose, but it did not exceed $\sim 15\%$ ID/g at all doses tested (Fig. 2B). Based on these data, a bsMAb dose of 6.0 nmol was selected for targeting 0.1 to 0.25 nmol of ^{68}Ga -IMP-288 to the tumor.

PET imaging

Five mice bearing an LS174T CEA-expressing tumor in the right flank and SK-RC 52, a CEA-negative tumor, in the left flank were administered 6.0 nmol ^{125}I -TF2 intravenously. After 16 hours, the mice received 5 MBq ^{68}Ga -IMP-288 (0.25 nmol, specific activity of 20 MBq/nmol). A separate group of three mice received the same amount of ^{68}Ga -IMP-288 alone, without pretargeting with TF2. PET/CT scans of the mice were acquired 1 hour after injection of ^{68}Ga -IMP-288.

The biodistribution of ^{125}I -TF2 and ^{68}Ga -IMP-288 in mice is shown in Fig. 3A. High uptake of the bsMab ($2.17 \pm 0.50\%$ ID/g) and peptide ($10.7 \pm 3.6\%$ ID/g) in the tumor was observed, with very low accretion in the normal tissues (tumor-to-blood ratio for ^{68}Ga -IMP-288: 64 ± 22). Most importantly, targeting of ^{68}Ga -IMP-288 in the CEA-negative tumor SK-RC 52 was very low ($0.35 \pm 0.35\%$ ID/g). Likewise, tumors that were not pretargeted with TF2 had a low uptake of ^{68}Ga -IMP-288 ($0.20 \pm 0.03\%$ ID/g), indicating that the specific accumulation of IMP-288 in the CEA-expressing LS174T tumor was derived from the prelocalization of the bsMab.

The specific uptake of ^{68}Ga -IMP-288 in the CEA-expressing tumor pretargeted with TF2 was clearly visualized in the PET image acquired 1 hour after injection, without any localization in the negative tumor (Fig. 3B). Uptake in the tumor was evaluated quantitatively by drawing regions of interest using a 50% threshold of maximum intensity. A region in the abdomen was used as background region. The tumor-to-background ratio in the image of the mouse that received TF2 and ^{68}Ga -IMP-288 was 38.2 at 1 hour.

In the next studies, two groups of five mice bearing a s.c. LS174T tumor in the right hind leg and a turpentine-induced inflammatory focus in the left thigh muscle were examined to assess the specificity of the pretargeting procedure compared with ^{18}F -FDG. Three days after the induction of the inflammatory lesion, one group of mice received 6.0 nmol TF2, followed 16 hours later by 5 MBq ^{68}Ga -IMP-288 (0.25 nmol). The other group received ^{18}F -FDG (5 MBq). Mice were fasted for 10 hours before the injection and anesthetized and kept warm at 37°C until euthanasia 1 hour after injection.

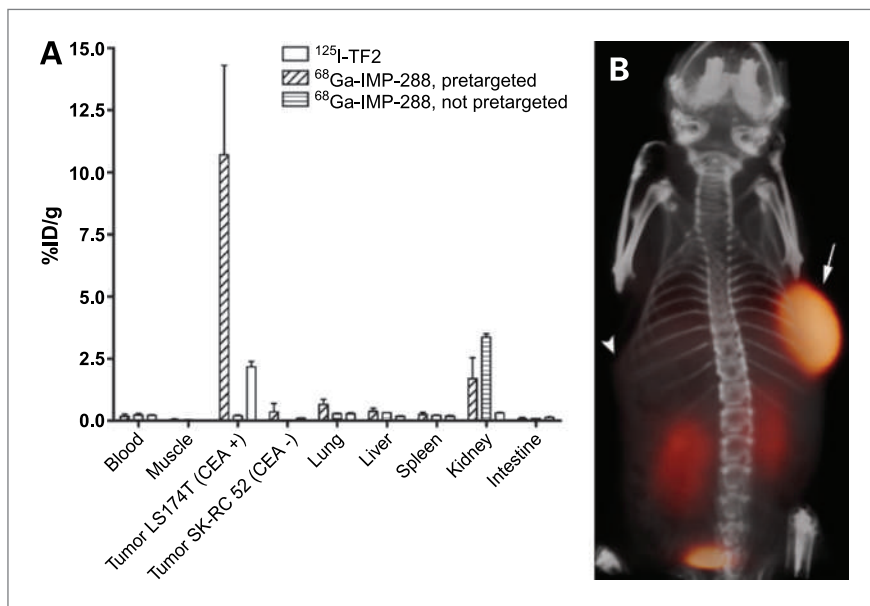
Figure 4A shows an example of a mouse that received the TF2-pretargeted ^{68}Ga -IMP-288, showing efficient

accretion of the radiolabeled peptide in the tumor, whereas the inflamed muscle was not visualized. In contrast, both tumor and inflammation were visible in the mice that received ^{18}F -FDG (Fig. 4B). In mice given ^{68}Ga -IMP-288, the tumor-to-inflamed tissue ratio by standardized uptake value analysis was 5.4 and the tumor-to-background ratio was 48. ^{18}F -FDG uptake had a tumor-to-inflamed muscle ratio of 0.83, and the tumor-to-background ratio was 2.4.

At necropsy, uptake of ^{68}Ga -IMP-288 measured in the inflamed muscle was only $0.72 \pm 0.20\%$ ID/g, but tumor uptake was $8.73 \pm 1.60\%$ ID/g ($P < 0.05$; Fig. 5). The tumor-to-blood ratio of ^{68}Ga -IMP-288 in these mice was 69.9 ± 32.3 , the inflamed muscle-to-blood ratio was 5.9 ± 2.9 , and the tumor-to-inflamed muscle ratio was 12.5 ± 2.1 . ^{18}F -FDG accreted efficiently in the tumor ($7.42 \pm 0.20\%$ ID/g; tumor-to-blood ratio, 6.24 ± 1.5 ; Fig. 5) but also accumulated substantially in the inflamed muscle ($4.07 \pm 1.13\%$ ID/g), with an inflamed muscle-to-blood ratio of 3.4 ± 0.5 and a tumor-to-inflamed muscle ratio of 1.97 ± 0.71 .

Finally, the pretargeted immuno-PET imaging method was tested using the ^{18}F -labeled peptide IMP-449. Five mice received 6.0 nmol TF2, followed 16 hours later by 5 MBq ^{18}F -IMP-449 (0.25 nmol). Three additional mice received 5 MBq ^{18}F -IMP-449 without prior administration of TF2, whereas two mice were injected with $\text{Al}[^{18}\text{F}]^{2+}$ (3 MBq). Uptake of ^{18}F -IMP-449 at 1 hour in tumors pretargeted with TF2 was high ($10.6 \pm 1.7\%$ ID/g; Fig. 6), whereas it was very low in the nonpretargeted mice ($0.45 \pm 0.38\%$ ID/g). $\text{Al}[^{18}\text{F}]^{2+}$ accumulated in the bone ($50.9 \pm 11.4\%$ ID/g), whereas uptake of IMP-449 peptide in the bone was very low ($0.54 \pm 0.2\%$ ID/g), indicating that ^{18}F -IMP-449 was stable *in vivo*. Importantly, the biodistribution of ^{18}F -IMP-449 in the TF2 pretargeted mice

Figure 3. A, biodistribution of 6.0 nmol ^{125}I -TF2 (0.37 MBq) and 0.25 nmol ^{68}Ga -IMP-288 (5 MBq) 1 h after i.v. injection of ^{68}Ga -IMP-288 in BALB/c nude mice with a s.c. LS174T and SK-RC 52 tumor. Values are given as means \pm SD ($n = 5$). B, three-dimensional volume rendering of PET/CT image of a BALB/c nude mouse with a s.c. LS174T CEA-expressing tumor in the right flank (arrow) and a s.c. SK-RC 52 tumor, a non-CEA-producing tumor, in the left flank (arrowhead), which received 6.0 nmol TF2 and 5 MBq ^{68}Ga -IMP-288 (0.25 nmol) i.v. with a 16-h interval, imaged 1 h after ^{68}Ga -IMP-288 injection.



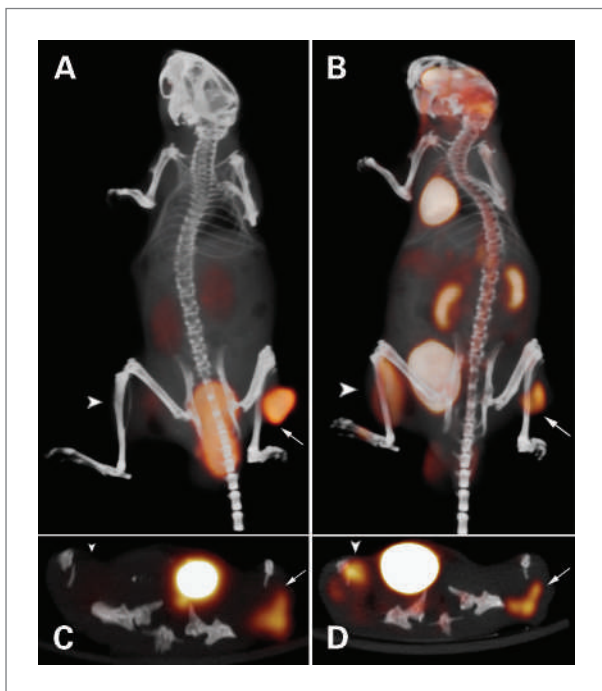


Figure 4. PET/CT images of a BALB/c nude mouse with a s.c. LS174T tumor (0.1 g) on the right hind leg (arrow) and an inflammation in the left thigh muscle (arrowhead), which received 5 MBq ^{18}F -FDG and, 1 d later, 6.0 nmol TF2 and 5 MBq ^{68}Ga -IMP-288 (0.25 nmol) with a 16-h interval. The animal was imaged 1 h after ^{18}F -FDG and ^{68}Ga -IMP-288 injections. The panel shows the three-dimensional volume rendering of the pretargeted immuno-PET scan (A) and the FDG-PET scan (B), and the transverse sections of the tumor region of the pretargeted immuno-PET scan (C) and the FDG-PET scan (D).

was very similar to that of ^{68}Ga -IMP-288, indicating the suitability for either of these radiolabeled agents for use in pretargeted PET imaging. Pretargeted immuno-PET images with ^{18}F -IMP-449 showed the same intensity in the tumor as those with ^{68}Ga -IMP-288, but the resolution of the ^{18}F images was better than the ^{68}Ga images (Fig. 7). The tumor-to-background ratio of the ^{18}F -IMP-449 signal was 66.

Discussion

Several important conclusions can be made from the present study. Pretargeting affords the possibilities of using antibody-based imaging techniques with short-lived radionuclides, such as ^{68}Ga and ^{18}F , which are ideally suited for PET imaging. Before the use of ^{18}F -FDG and PET imaging, radiolabeled antibodies were being developed commercially for the detection of colorectal, ovarian, lung, and prostate cancers using single-photon emission computed tomography imaging systems (23). However, all of these imaging methods suffered from relatively poor contrast even when radiolabeled antibody fragments were used (24). Unquestionably, the advent of ^{18}F -FDG provided the necessary platform for the development of molecular imaging based on the newly de-

veloped PET imaging systems, and as a result, most of these antibody-imaging agents have been withdrawn from the market. Since then, molecular engineering has fostered a new era for antibodies, making it possible to craft many different forms with more favorable blood clearance and targeting potential (25). Still, many of these new constructs require considerable time for good tumor uptake and contrast to develop, and therefore, radionuclides with longer half-lives, such as ^{64}Cu and ^{124}I , are often used. For example, Cai et al. (26) reported an attempt to use a directly radiolabeled ^{18}F -anti-CEA diabody for imaging. Although this type of construct has very favorable pharmacokinetic properties, maximum tumor uptake in LS174T xenografts obtained at 1 hour after injection was only 2.7% ID/g, along with 2.0% ID/g in the blood and higher uptake in the other major organs. Low but favorable tumor-to-tissue ratios required 4 to 6 hours to develop. ^{124}I has been used with directly radiolabeled antibody constructs for a large part because radioiodine will not be retained in normal tissues, and thus, more reasonable tumor-to-tissue ratios can be achieved than with a radiometal (27). However, the added expense and relatively poor imaging properties of this radionuclide are considerable barriers to the development of products based on ^{124}I . As our studies show, the short physical half-life of ^{18}F and ^{68}Ga can be used effectively in pretargeting to enhance detection sensitivity.

The half-life of ^{68}Ga is well matched to the kinetics of the IMP-288 peptide in the pretargeting system. ^{68}Ga can be eluted twice daily from a $^{68}\text{Ge}/^{68}\text{Ga}$ generator, avoiding the need for an on-site cyclotron. However, the high

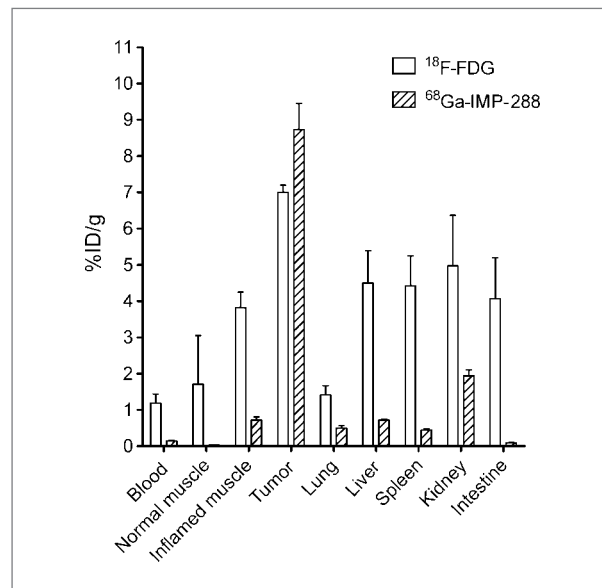


Figure 5. Biodistribution of 5 MBq FDG and 5 MBq ^{68}Ga -IMP-288 (0.25 nmol) 1 h after injection, following pretargeting with 6.0 nmol TF2 in BALB/c nude mice with a s.c. CEA-expressing LS174T tumor. Values are given as means \pm SD ($n = 5$).

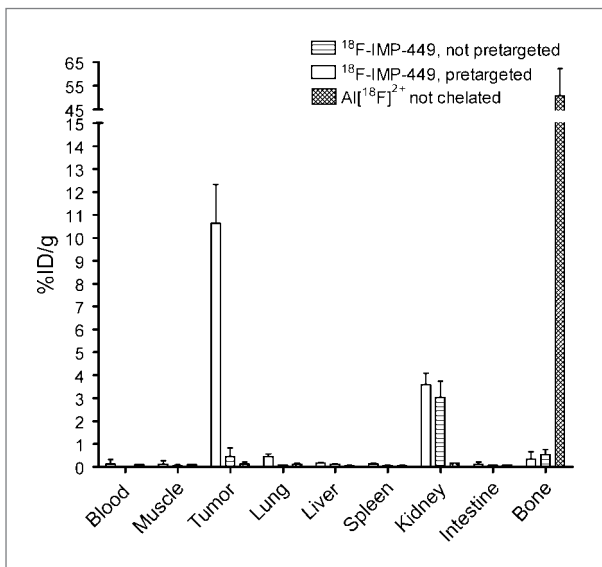


Figure 6. Biodistribution of 0.25 nmol ¹⁸F-IMP-449 (5 MBq) 1 h after injection, following pretargeting with 6.0 nmol TF2 16 h earlier, biodistribution of ¹⁸F-IMP-449 without pretargeting, or biodistribution of Al[¹⁸F]²⁺ in BALB/c nude mice with a s.c. CEA-expressing LS174T tumor. Values are given as means ± SD.

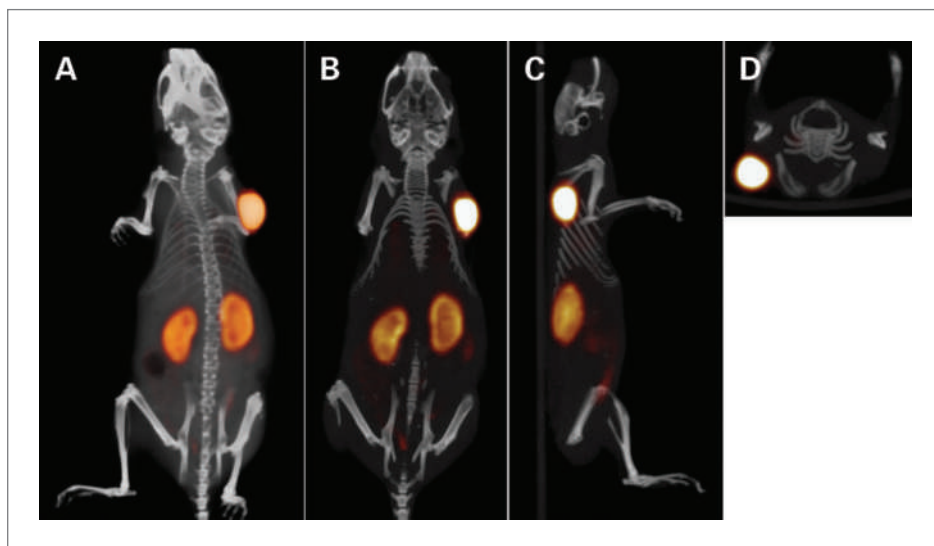
energy of the positrons emitted by ⁶⁸Ga (1.9 MeV) limits the spatial resolution of the acquired images to 3 mm, whereas the intrinsic resolution of the micro-PET system is as low as 1.5 mm (22). In the clinical setting, the penetration range of ⁶⁸Ga positrons does not reduce the resolution of the images. For these studies, the procedure to label IMP-288 with ⁶⁸Ga was optimized, resulting in a one-step labeling technique. We found that purification on a C18/HLB cartridge was required to remove the ⁶⁸Ga colloid that is inevitably formed when the peptide was labeled at specific activities exceeding

150 GBq/nmol at 95°C. ⁶⁸Ga colloid accumulates in tissues of the reticuloendothelial system (liver, spleen, and bone marrow), deteriorating image quality, but it could be effectively reduced by rapid purification on a C18 cartridge. Radiolabeling and purification for administration could be accomplished within 45 minutes.

¹⁸F, the most widely used radionuclide in PET, has an even more favorable half-life for pretargeted PET imaging ($t_{1/2} = 110$ minutes). Therefore, in this study, the NOTA-conjugated peptide IMP-449 was labeled with ¹⁸F, as recently described by McBride et al. (13). We showed that this method produces a preparation that is stable *in vivo*. Similar to labeling with ⁶⁸Ga, it is a one-step procedure, which currently requires high-performance liquid chromatography purification to remove the unlabeled peptide to enhance specific activity. Labeling yield was as high as 50%. Interestingly, the biodistribution of ¹⁸F-IMP-449 was similar to that of ⁶⁸Ga-labeled IMP-288, suggesting that the new labeling method using NOTA to chelate Al[¹⁸F]²⁺ turns the ¹⁸F label into a residualizing radionuclide. Presumably, the peptide undergoes proteolytic degradation in the lysosomes, and its radiolabeled catabolite, containing Al[¹⁸F]²⁺-NOTA, is trapped in the lysosomes, as has been described for radiometals.

In contrast to FDG-PET, pretargeted radioimmunodetection is a tumor-specific imaging modality. Although a high sensitivity and specificity for FDG-PET in detecting recurrent colorectal cancer lesions has been reported in patients (28), FDG-PET images could lead to diagnostic dilemmas in discriminating malignant from benign, highly metabolic lesions, such as inflammation. Earlier studies in animal models have highlighted the improvements that an antibody-based pretargeting procedure can provide in comparison with ¹⁸F-FDG, focusing primarily on its enhanced sensitivity (12). In this study, we addressed the specificity of pretargeting in relation to its

Figure 7. Static PET/CT imaging study of a BALB/c nude mouse with a s.c. LS174T tumor (0.1 g) on the right side, which received 6.0 nmol TF2 and 0.25 nmol ¹⁸F-IMP-449 (5 MBq) i.v. with a 16-h interval. The animal was imaged 1 h after injection of ¹⁸F-IMP-449. The panel shows the three-dimensional volume rendering (posterior view; A) and cross-sections at the tumor region [coronal (B), sagittal (C), and transversal (D)].



ability to discriminate inflammatory lesions from cancer. As expected, ^{18}F -FDG had high uptake in the tumor, but this was only 2-fold higher than the uptake in the inflammatory lesion. In contrast, tumor uptake was at least 10-fold higher in the tumor compared with the inflammatory lesion with the antibody-based pretargeting method. Additionally, we showed that pretargeting specifically localizes in the intended target, with a 30 times higher concentration in the antigen-positive tumor than in a negative tumor. Thus, with evidence for appreciable improvements in both sensitivity and specificity, bsMAB-based pretargeting procedures could provide important new tools for detecting cancer.

This pretargeting method is a two-step process that first requires the administration of the unlabeled bsMAB. Rather than using a clearing agent, the bsMABs are designed in a manner to minimize their residence time in the blood. Despite its size equaling that of an IgG (i.e., 157×10^3 Da), TF2 is cleared very quickly. The long circulatory half-life of IgG is only partly determined by its large size and is mainly due to the presence of the $\text{C}_{\text{H}2}$ domain, which enables recycling via FcRn receptors (29). It has been shown that $\text{C}_{\text{H}2}$ domain-deleted variants of IgG (121×10^3 Da) clear much faster from the blood than intact IgG (30, 31). TF2 is an engineered trivalent antibody derived from three Fab fragments and lacks any $\text{C}_{\text{H}2}$ domain.

These studies also provide new insights into this pretargeting method. Earlier studies examined the effects of increasing the bsMAB with a fixed amount of the peptide in mice with GW-39 human colonic tumors. It was reported that beyond a 10:1 molar ratio of bsMAB-peptide, the amount of peptide that could be delivered to the tumor did not increase (32). Using a low peptide dose level (0.01 nmol), we found that tumor uptake in the LS174T model increased as the moles of bsMAB were increased from 0.1 to 1 nmol, reaching a maximum uptake of $\sim 25\%$ ID/g with 1 nmol TF2 (i.e., a 100:1 molar ratio) with minimal changes in blood and normal tissue uptake.

Compared with earlier studies, several factors contributed to the need for injecting considerably more hapten peptide in these studies, including the size and age of the

^{68}Ga generator, yields after purification, and the natural decay of the product that required a minimum of 5 MBq to be administered for imaging. Thus, a separate biodistribution study was done to examine a similar dose response with 10-fold more IMP-288 (0.1 nmol). Despite administering increasing amounts of TF2 at the same molar ratios used with 0.01 nmol of IMP-288, tumor uptake remained highly favorable but remained at a constant level of $\sim 15\%$ ID/g over a TF2 dose range of 1 to 10 nmol. TF2 tumor uptake showed a constant level of $\sim 3\%$ ID/g over a dose range from 0.1 to 1.0 nmol, but at the 2.5 nmol dose, the percent uptake began to decline, reducing to $\sim 1\%$ ID/g at 10 nmol. Consequently, at the high IMP-288 dose (0.1 nmol), increasing the TF2 dose did not result in higher tumor uptake of radiolabeled IMP-288. These data suggest that at TF2 doses exceeding 2.5 nmol, saturation of CEA in the tumor (with TF2) occurs. Thus, in pretargeting, exceptionally favorable targeting at lower specific activities can be achieved, but a higher fractional uptake results at its highest specific activity.

In conclusion, pretargeted immuno-PET with an anti-CEA bsMAB and a ^{68}Ga - or ^{18}F -labeled hapten peptide is a rapid, highly specific, and sensitive imaging modality for the detection CEA-positive tumors.

Disclosure of Potential Conflicts of Interest

W.J. McBride, D.M. Goldenberg, E.A. Rossi, and C-H. Chang are employed by or have financial interest in Immunomedics, Inc. and/or IBC Pharmaceuticals, Inc. The other authors disclosed no potential conflicts of interest.

Grant Support

Dutch Cancer Society (Koningin Wilhelmina Fonds Kankerbestrijding) grant KUN 2008-4038 and NIH grant 1 R43 EB003751 from the National Institute of Biomedical Imaging and Bioengineering.

The costs of publication of this article were defrayed in part by the payment of page charges. This article must therefore be hereby marked *advertisement* in accordance with 18 U.S.C. Section 1734 solely to indicate this fact.

Received 09/15/2009; revised 01/18/2010; accepted 01/25/2010; published OnlineFirst 03/30/2010.

References

- Jain RK. Physiological barriers to delivery of monoclonal antibodies and other macromolecules in tumors. *Cancer Res* 1990;50:814-9s.
- Sharkey RM, Karacay H, Cardillo TM, et al. Improving the delivery of radionuclides for imaging and therapy of cancer using pretargeting methods. *Clin Cancer Res* 2005;11:7109-21s.
- Reardan DT, Meares CF, Goodwin DA, et al. Antibodies against metal chelates. *Nature* 1985;316:265-8.
- Boerman OC, van Schaijk FG, Oyen WJ, Corstens FH. Pretargeted radioimmunotherapy of cancer: progress step by step. *J Nucl Med* 2003;44:400-11.
- Chang CH, Sharkey RM, Rossi EA, et al. Molecular advances in pretargeting radioimmunotherapy with bispecific antibodies. *Mol Cancer Ther* 2002;1:553-63.
- Sharkey RM, Cardillo TM, Rossi EA, et al. Signal amplification in molecular imaging by pretargeting a multivalent, bispecific antibody. *Nat Med* 2005;11:1250-5.
- Le Doussal JM, Martin M, Gautherot E, Delaage M, Barbet J. *In vitro* and *in vivo* targeting of radiolabeled monovalent and divalent haptens with dual specificity monoclonal antibody conjugates: enhanced divalent hapten affinity for cell-bound antibody conjugate. *J Nucl Med* 1989;30:1358-66.
- Karacay H, McBride WJ, Griffiths GL, et al. Experimental pretargeting studies of cancer with a humanized anti-CEA \times murine anti-[In-DTPA] bispecific antibody construct and a (99m)Tc-/(188)Re-labeled peptide. *Bioconjug Chem* 2000;11:842-54.
- Griffiths GL, Chang CH, McBride WJ, et al. Reagents and methods for PET using bispecific antibody pretargeting and ^{68}Ga -radiolabeled bivalent hapten-peptide-chelate conjugates. *J Nucl Med* 2004;45:30-9.
- McBride WJ, Zanzonico P, Sharkey RM, et al. Bispecific antibody pretargeting PET (immunoPET) with an ^{124}I -labeled hapten-peptide. *J Nucl Med* 2006;47:1678-88.

11. Sharkey RM, McBride WJ, Karacay H, et al. A universal pretargeting system for cancer detection and therapy using bispecific antibody. *Cancer Res* 2003;63:354–63.
12. Sharkey RM, Karacay H, Vallabhajosula S, et al. Metastatic human colonic carcinoma: molecular imaging with pretargeted SPECT and PET in a mouse model. *Radiology* 2008;246:497–507.
13. McBride WJ, Sharkey RM, Karacay H, et al. A novel method of ^{18}F radiolabeling for PET. *J Nucl Med* 2009;50:991–8.
14. Morel A, Darmon M, Delaage M. Recognition of imidazole and histamine derivatives by monoclonal antibodies. *Mol Immunol* 1990;27:995–1000.
15. Sharkey RM, Goldenberg DM, Goldenberg H, et al. Murine monoclonal antibodies against carcinoembryonic antigen: immunological, pharmacokinetic, and targeting properties in humans. *Cancer Res* 1990;50:2823–31.
16. Goldenberg DM, Rossi EA, Sharkey RM, McBride WJ, Chang CH. Multifunctional antibodies by the Dock-and-Lock method for improved cancer imaging and therapy by pretargeting. *J Nucl Med* 2008;49:158–63.
17. Rossi EA, Goldenberg DM, Cardillo TM, McBride WJ, Sharkey RM, Chang CH. Stably tethered multifunctional structures of defined composition made by the dock and lock method for use in cancer targeting. *Proc Natl Acad Sci U S A* 2006;103:6841–6.
18. Lindmo T, Boven E, Cuttitta F, Fedorko J, Bunn PA, Jr. Determination of the immunoreactive fraction of radiolabeled monoclonal antibodies by linear extrapolation to binding at infinite antigen excess. *J Immunol Methods* 1984;72:77–89.
19. Fraker PJ, Speck JC, Jr. Protein and cell membrane iodinations with a sparingly soluble chloroamide, 1,3,4,6-tetrachloro-3a,6a-diphrenylglycoluril. *Biochem Biophys Res Commun* 1978;80:849–57.
20. Ebert T, Bander NH, Finstad CL, Ramsawak RD, Old LJ. Establishment and characterization of human renal cancer and normal kidney cell lines. *Cancer Res* 1990;50:5531–6.
21. Van der Laken CJ, Boerman OC, Oyen WJ, et al. *In vivo* expression of interleukin-1 receptors during various experimentally induced inflammatory conditions. *J Infect Dis* 1998;177:1398–401.
22. Visser EP, Disselhorst JA, Brom M, et al. Spatial resolution and sensitivity of the Inveon small-animal PET scanner. *J Nucl Med* 2009;50:139–47.
23. Van de Wiele C, Revets H, Mertens N. Radioimmunoimaging. Advances and prospects. *Q J Nucl Med Mol Imaging* 2004;48:317–25.
24. Goldenberg DM. Perspectives on oncologic imaging with radiolabeled antibodies. *Cancer* 1997;80:2431–5.
25. Wu AM, Olafsen T. Antibodies for molecular imaging of cancer. *Cancer J* 2008;14:191–7.
26. Cai W, Olafsen T, Zhang X, et al. PET imaging of colorectal cancer in xenograft-bearing mice by use of an ^{18}F -labeled T84.66 anti-carcinoembryonic antigen diabody. *J Nucl Med* 2007;48:304–10.
27. Sharkey RM, Motta-Hennessy C, Pawlyk D, Siegel JA, Goldenberg DM. Biodistribution and radiation dose estimates for yttrium- and iodine-labeled monoclonal antibody IgG and fragments in nude mice bearing human colonic tumor xenografts. *Cancer Res* 1990;50:2330–6.
28. Huebner RH, Park KC, Shepherd JE, et al. A meta-analysis of the literature for whole-body FDG PET detection of recurrent colorectal cancer. *J Nucl Med* 2000;41:1177–89.
29. Ghetie V, Ward ES. FcRn: the MHC class-I-related receptor that is more than an IgG transporter. *Immunol Today* 1997;18:592–8.
30. Chinn PC, Morena RA, Santoro DA, et al. Pharmacokinetics and tumor localization of (^{111}In) -labeled HuCC49 $\Delta\text{C}(\text{H})2$ in BALB/c mice and athymic murine colon carcinoma xenograft. *Cancer Biother Radiopharm* 2006;21:106–6.
31. Slavin-Chiorini DC, Kashmiri SV, Lee HS, et al. A CDR-grafted (humanized) domain-deleted antitumor antibody. *Cancer Biother Radiopharm* 1997;12:305–16.
32. Sharkey RM, Karacay H, Richel H, et al. Optimizing bispecific antibody pretargeting for use in radioimmunotherapy. *Clin Cancer Res* 2003;9:3897–913S.

Molecular Cancer Therapeutics

Pretargeted Immuno–Positron Emission Tomography Imaging of Carcinoembryonic Antigen–Expressing Tumors with a Bispecific Antibody and a ^{68}Ga - and ^{18}F -Labeled Hapten Peptide in Mice with Human Tumor Xenografts

Rafke Schoffelen, Robert M. Sharkey, David M. Goldenberg, et al.

Mol Cancer Ther 2010;9:1019-1027. Published OnlineFirst March 30, 2010.

Updated version Access the most recent version of this article at:
doi:[10.1158/1535-7163.MCT-09-0862](https://doi.org/10.1158/1535-7163.MCT-09-0862)

Cited articles This article cites 32 articles, 15 of which you can access for free at:
<http://mct.aacrjournals.org/content/9/4/1019.full#ref-list-1>

Citing articles This article has been cited by 7 HighWire-hosted articles. Access the articles at:
<http://mct.aacrjournals.org/content/9/4/1019.full#related-urls>

E-mail alerts [Sign up to receive free email-alerts](#) related to this article or journal.

Reprints and Subscriptions To order reprints of this article or to subscribe to the journal, contact the AACR Publications Department at pubs@aacr.org.

Permissions To request permission to re-use all or part of this article, use this link
<http://mct.aacrjournals.org/content/9/4/1019>.
Click on "Request Permissions" which will take you to the Copyright Clearance Center's (CCC) Rightslink site.